

Lattice positions of Sn in Cu₂ZnSnS₄ nanoparticles and thin films studied by synchrotron X-ray absorption near edge structure analysis

E. Zillner, A. Paul, J. Jutimoosik, S. Chandarak, T. Monnor, S. Rujirawat, R. Yimnirun, X. Z. Lin, A. Ennaoui, Th. Dittrich, and M. Lux-Steiner

Citation: *Applied Physics Letters* **102**, 221908 (2013); doi: 10.1063/1.4809824

View online: <http://dx.doi.org/10.1063/1.4809824>

View Table of Contents: <http://scitation.aip.org/content/aip/journal/apl/102/22?ver=pdfcov>

Published by the [AIP Publishing](#)

Articles you may be interested in

[Investigation of combinatorial coevaporated thin film Cu₂ZnSnS₄ \(II\): Beneficial cation arrangement in Cu-rich growth](#)

J. Appl. Phys. **115**, 173503 (2014); 10.1063/1.4871665

[Strain tuning of native defect populations: The case of Cu₂ZnSn\(S,Se\)₄](#)

APL Mat. **2**, 012110 (2014); 10.1063/1.4863076

[Model of native point defect equilibrium in Cu₂ZnSnS₄ and application to one-zone annealing](#)

J. Appl. Phys. **114**, 124501 (2013); 10.1063/1.4819206

[Determination of secondary phases in kesterite Cu₂ZnSnS₄ thin films by x-ray absorption near edge structure analysis](#)

Appl. Phys. Lett. **99**, 262105 (2011); 10.1063/1.3671994

[Analysis of lattice site occupancy in kesterite structure of Cu₂ZnSnS₄ films using synchrotron radiation x-ray diffraction](#)

J. Appl. Phys. **110**, 074511 (2011); 10.1063/1.3642993

The logo for the Journal of Applied Physics (AIP) is displayed in a white font on an orange background. The letters 'AIP' are large and bold, followed by a vertical bar and the words 'Journal of Applied Physics' in a smaller font.

Journal of Applied Physics is pleased to announce **André Anders** as its new Editor-in-Chief

Lattice positions of Sn in $\text{Cu}_2\text{ZnSnS}_4$ nanoparticles and thin films studied by synchrotron X-ray absorption near edge structure analysis

E. Zillner,^{1,a)} A. Paul,² J. Jutimoosik,³ S. Chandarak,³ T. Monnor,³ S. Rujirawat,³ R. Yimnirun,³ X. Z. Lin,¹ A. Ennaoui,¹ Th. Dittrich,¹ and M. Lux-Steiner¹

¹Helmholtz-Zentrum Berlin für Materialien und Energie, Hahn-Meitner Platz 1, 14109 Berlin, Germany

²Technische Universität München, Physik Department E21, James-Franck-Straße 1, 85748 Garching, Germany

³School of Physics, Institute of Science, Suranaree University of Technology, and NANOTEC-SUT Center of Excellence on Advanced Functional Nanomaterials, Nakhon Ratchasima 30000, Thailand

(Received 11 March 2013; accepted 23 May 2013; published online 6 June 2013)

Lattice positions of Sn in kesterite $\text{Cu}_2\text{ZnSnS}_4$ and Cu_2SnS_3 nanoparticles and thin films were investigated by XANES (x-ray absorption near edge structure) analysis at the S K-edge. XANES spectra were analyzed by comparison with simulations taking into account anti-site defects and vacancies. Annealing of $\text{Cu}_2\text{ZnSnS}_4$ nanoparticle thin films led to a decrease of Sn at its native and defect sites. The results show that XANES analysis at the S K-edge is a sensitive tool for the investigation of defect sites, being critical in kesterite thin film solar cells. © 2013 AIP Publishing LLC. [<http://dx.doi.org/10.1063/1.4809824>]

Kesterite type $\text{Cu}_2\text{ZnSnS}_4$ is a semiconductor with a band gap of about 1.5 eV and a large absorption coefficient what makes this material very interesting for applications in thin film solar cells.¹ Despite the fact that relatively high energy conversion efficiencies have been already reached for solar cells with kesterite type absorbers,^{2–6} little is known about the nature of defects in related quaternary compounds. There is generally a large probability for formation of defects such as anti-site defects and vacancies in quaternary compounds. Especially, variations of the occupation of lattice sites in kesterite type absorbers seem to be crucial for the performance of solar cells with related absorbers. For example, relatively high energy conversion efficiencies could be only achieved for $\text{Cu}_2\text{ZnSnS}_4$ solar cells within a quite narrow region of Cu-poor and Zn-rich compositions.^{1,4,7–9} Further, annealing of thin films with kesterite type nanoparticles is very important for the formation of $\text{Cu}_2\text{ZnSnS}_4$ absorbers. Annealing changes the occupation of lattice sites and therefore the formation of defect sites in a $\text{Cu}_2\text{ZnSnS}_4$ crystallite. Guo *et al.*, for example, observed a loss of Sn during annealing under Se vapor.⁶ Tin is multivalent and can be a trap, donor, or acceptor depending on the lattice position in $\text{Cu}_2\text{ZnSnS}_4$. Simulations predict different energies for the transition between Sn^{+II} and Sn^{+IV} depending on the lattice position and the parameter and model used.^{10,11} A transition within in the band gap would lead to a defect state in the semiconductor.¹⁰ According to Biswas *et al.*, Sn forms a defect only on the intrinsic Zn position,¹⁰ whereas according to Walsh *et al.*, Sn also forms a deep defect on the Cu position.¹¹ A more detailed analysis of the behavior of Sn atoms in $\text{Cu}_2\text{ZnSnS}_4$ can be useful for getting a deeper understanding of defects in kesterite type absorbers and for improving the performance of thin film solar cells based on $\text{Cu}_2\text{ZnSnS}_4$.

$\text{Cu}_2\text{ZnSnS}_4$ crystallizes in a kesterite lattice^{12,13} (space group $\bar{I}4$, $a = 5.428 \text{ \AA}$; $c = 10.846 \text{ \AA}$) as shown in Figure 1. Sulfur atoms occupy the 8g lattice positions. Copper atoms

occupy the 2c and 2a lattice positions, whereas tin and zinc atoms occupy the 2b and 2d lattice positions, respectively. Attention has been paid to the Cu-Zn anti-site defect when copper atoms occupy 2d positions and zinc atoms occupy 2c positions (investigations by neutron diffraction¹⁴ and synchrotron x-ray diffraction¹⁵). XANES at the S K-edge has been applied to determine the volume fraction of ZnS in the $\text{Cu}_2\text{ZnSnS}_4$ layer which is dependent upon the Sn/Zn ratio by fitting XANES spectra with a linear combination of reference spectra of pure $\text{Cu}_2\text{ZnSnS}_4$ and ZnS.¹⁶

This work is aimed for the analysis of anti-site defects and vacancies of Sn in kesterite type $\text{Cu}_2\text{ZnSnS}_4$ by a method suitable for monitoring nanoparticles and thin film layers. The influence of defects in kesterite, which are potential traps, on the performance of kesterite solar cells has to be studied to reach high efficiencies.

In this work, XANES (x-ray absorption near edge structure) at the S K-edge has been applied as a relatively fast and reliable method to characterize these defects. The sulfur atom in kesterite $\text{Cu}_2\text{ZnSnS}_4$ occupies the 8g position and is surrounded by Cu (2c and 2a), Sn (2b), and Zn (2d) atoms in the first shell (see Figure 1). XANES at the S K-edge is therefore sensitive to the 2a, 2b, 2c, and 2d positions. As a remark, EXAFS (extended x-ray absorption fine structure) is also a well-known method for the analysis of neighbor atoms in lattice positions. However, XANES is a much faster method for measurements in the fluorescence mode which is required for the investigation of thin films.

The $\text{Cu}_2\text{ZnSnS}_4$ nanoparticles were prepared by two different routes. The first preparation route was via a colloidal synthesis, which relied on the reaction of Cu_2SnS_3 ($d = 10 \text{ nm}$) and ZnS ($d = 5 \text{ nm}$) nanoparticles. This resulted in kesterite $\text{Cu}_2\text{ZnSnS}_4$ nanoparticles with a diameter of $14 \pm 3 \text{ nm}$. The Cu_2SnS_3 nanoparticles crystallized in the stannite structure. We employed a second preparation route of $\text{Cu}_2\text{ZnSnS}_4$ nanoparticles synthesis which is a one pot technique. The synthesis works by a high-temperature arrested precipitation in the coordinating solvent after

^{a)}elisabeth.zillner@helmholtz-berlin.de

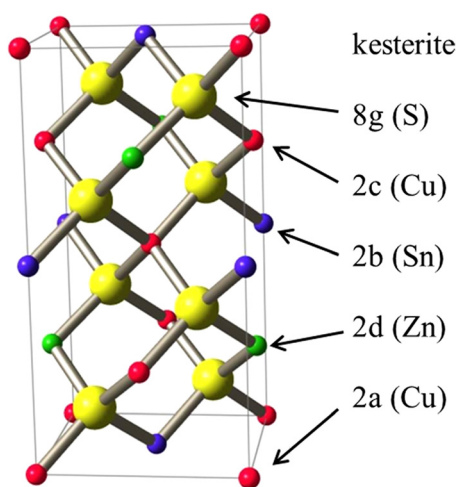


FIG. 1. Kesterite structure of $\text{Cu}_2\text{ZnSnS}_4$ with nomenclature and occupation of lattice sites.

Steinhagen, but at lower temperatures of 240°C .^{17,18} The resulting $\text{Cu}_2\text{ZnSnS}_4$ nanoparticles also had a kesterite structure and a diameter of 18 ± 4 nm. Thin layers of these nanoparticles were prepared by a drop cast method. The structure of the nanoparticles was verified by X-ray diffraction measurements.

XANES measurements were performed at the x-ray absorption spectroscopy beamline (BL-8) of the Siam Photon Source (electron energy of 1.2 GeV, beam current 80–120 mA), Synchrotron Light Research Institute in Thailand. A double crystal monochromator InSb (111) was used to adjust the energy of the synchrotron x-ray beam with 0.20 eV energy steps. For measurements in the fluorescent mode, the signal was detected with a 13-component Ge detector. In transmission mode of measurements, we use ion chambers. X-ray intensities were recorded using two 10 cm long ion-chambers placed before and after the sample to record incoming and transmission X-ray intensities. Both ion-chambers were filled with 63 kPa N_2 gas. The normalization of the data was performed using the package ATHENA.¹⁹

Samples for transmission measurements consisted of a homogeneous layer of dried nanoparticle powder in between two sheets of Kapton[®] tape. The thickness of the powder layers was optimized to give an appropriate edge jump.

XANES spectra were simulated using the FEFF 8.2 code²⁰ based on *ab-initio* multiple scattering calculations for structures with varied occupations of lattice sites. The simulation was based on Hedin–Lundqvist self-energy without consideration of an edge shift and no exponential broadening. An amplitude reduction factor $S_0^2 = 0.5$ and a maximum k-value of 5 was used for the simulation. Full multiple scattering was considered within a radius of 6 \AA surrounding the central sulfur atom, considering thus scattering in the first 5 shells.

A XANES spectrum was measured in the transmission mode on $\text{Cu}_2\text{ZnSnS}_4$ nanoparticles synthesized by a reaction of Cu_2SnS_3 and ZnS nanoparticles (Figure 2). As a remark, measurements in the fluorescence mode gave the same spectra with a lower signal to noise ratio for the same accumulation times.

For comparison, XANES on Cu_2SnS_3 precursor nanoparticles was measured. In stannite Cu_2SnS_3 , the 4d and 2b

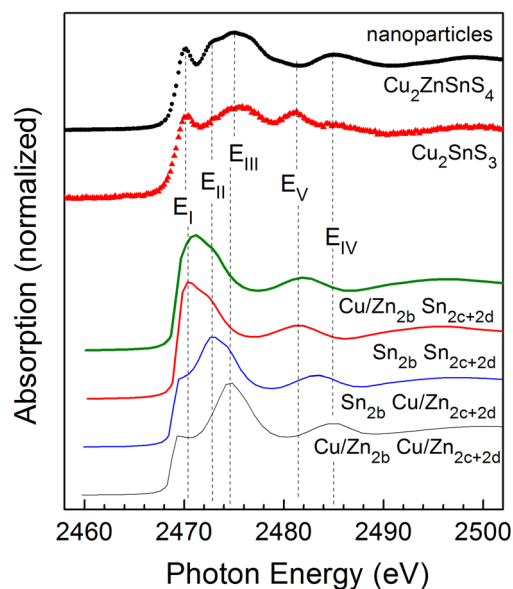


FIG. 2. Measured (symbols) and simulated (lines) normalized XANES spectra at the S K-edge of $\text{Cu}_2\text{ZnSnS}_4$ (black circles) and Cu_2SnS_3 (red triangles) nanoparticles and of kesterite type lattice structures with varied positions of Sn atoms: Cu and Zn replace Sn at 2b site and Cu and Zn at 2c and 2d sites (thinnest black line); Sn at 2b site and Cu and Zn at 2c and 2d sites (thin blue line); Sn at 2b site and Sn replace Cu and Zn at 2c and 2d sites (thick red line); Cu and Zn replace Sn at 2b site and Sn replace Cu and Zn at 2c and 2d sites (thickest green line). The baselines of the spectra are shifted.

positions are partially occupied by Cu and Sn.²¹ The 4d position in stannite is equal to the 2c and 2d position in kesterite which is occupied by Cu and Zn, respectively (see Figure 1). The 2b position in kesterite is occupied by Sn. Therefore, upon reaction of Cu_2SnS_3 with ZnS, the Sn should move out of the 4d position into the 2b position, whereas the Cu should leave the 2b site and move into the 2c position.

The XANES spectra of $\text{Cu}_2\text{ZnSnS}_4$ and Cu_2SnS_3 nanoparticles not only show some similar features but also show some clear differences. Four main peaks were found in the XANES spectrum of $\text{Cu}_2\text{ZnSnS}_4$ nanoparticles at 2470 eV (E_I), 2473 eV (E_{II}), 2475 eV (E_{III}), and 2485 eV (E_{IV}). A peak at 2481 eV (E_V) was found in the XANES spectrum of Cu_2SnS_3 in addition to the E_{I-IV} peaks found in XANES spectra of $\text{Cu}_2\text{ZnSnS}_4$ nanoparticles. Note that the shoulder at E_{II} was missing in the spectrum of Cu_2SnS_3 .

A classification of certain peak positions in XANES spectra with respect to the occupation of lattice sites is desired for thin film analysis. From the simulation results, it has been observed that the occupations of Cu and Zn are hardly distinguished in the XANES analysis, partly due to the fact that the atomic numbers of Cu and Zn are very close and Cu^+ and Zn^{2+} having similar symmetry and electron configuration in the input crystal structure. A similar trend has been observed for indium oxynitride alloys by T-Thienprasert *et al.*²² This behavior is indicated as Cu/Zn for any site occupied with Cu or Zn. Furthermore, the 2c and 2d positions are very similar and do not cause differences in the simulated XANES spectra.

In Figure 2, the results of the simulations with different occupations of the critical 2b and 2c + 2d sites are plotted. The nomenclatures Cu/Zn_{2b} Cu/Zn_{2c+2d} , Sn_{2b} Cu/Zn_{2c+2d} , Sn_{2b} Sn_{2c+2d} , and Cu/Zn_{2b} Sn_{2c+2d} are related to the atoms

occupying the indicated lattice sites. The peaks at E_{III} and E_{IV} correlate very well with the peaks at 2475 and 2485 eV of the simulated spectrum with Cu/Zn_{2b} Cu/Zn_{2c+2d} occupation.

The peak at E_{II} appeared only in the simulated XANES spectrum with Sn_{2b} Cu/Zn_{2c+2d} occupation which corresponds to the stoichiometric kesterite structure. The E_V peak at 2481 eV appeared in the simulated XANES spectra with Sn_{2b} Sn_{2c+2d} and Cu/Zn_{2b} Sn_{2c+2d} occupations. It can be concluded that the E_V peak is related to the occupation of 2c + 2d sites by Sn atoms.

However, the E_I peak is difficult to be classified by the XANES simulations. The first peak of the simulations with Sn on the 2c + 2d position fits energetically with E_I . However, the peak in the simulation is much broader and E_I does not correlate with E_V , as E_I is present in both nanoparticle samples and E_V only in Cu_2ZnSnS_3 . The simulation where Cu/Zn occupied the native Sn site (2b) also shows a small peak in the range of 2470 eV. Therefore, E_I was correlated with Cu/Zn on the 2b site. The slight differences between measurements and simulation can be explained by slight local disturbances in the lattice, which were not considered in XANES simulations.

The disappearance of the E_V peak present in the XANES spectrum of Cu_2ZnSnS_3 and the appearance of the E_{II} peak after reaction with ZnS is a result of the shift of Sn atoms from the 2c + 2d sites into its native position in kesterites, i.e. the 2b site. E_I however also indicates a certain amount of Cu/Zn in the 2b position. Therefore, anti-site defects in Cu_2ZnSnS_4 were present and the Cu_2ZnSnS_4 nanoparticles were Sn deficient.

Apart from anti-site defects also vacancies can lead to electron and hole traps in kesterite structures.¹¹ To see the influences of vacancies on near edge X-ray absorption, simulations with 2a, 2b, and 2c + 2d vacancies were performed and have been shown in Figure 3. The vacancies generally cause a shift of the peaks to higher energies and a peak around 2470 eV evolves. The strongest shift is caused by vacancies on the 2b site, whereas the most pronounced peak at 2470 eV is caused by the 2c + 2d vacancies. Note that the simulation with the Sn, the 2b vacancy is very similar to the

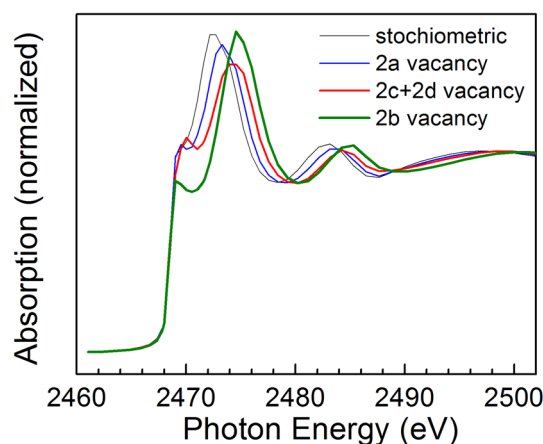


FIG. 3. Simulated XANES spectra at the S K-edge of Cu_2ZnSnS_4 with a stoichiometric structure (thinnest black line) and vacancies at the 2a (thin blue line), the 2c + 2d (thick red line), and the 2b (thickest green line) site.

simulation with Cu/Zn_{2b} Cu/Zn_{2c+2d} . Therefore, it cannot be distinguished between a Cu/Zn anti-site defect and a vacancy on the 2b position.

The analysis of the peak positions in XANES spectra can be used to monitor changes in the occupation of lattice sites during the phase transformation of precursor nanoparticles into kesterites and/or during further processing such as annealing, sulfurization or selenization. As an example, Figure 4 shows XANES spectra of thin films of kesterite nanoparticles deposited by drop casting on substrates (Figure 4(a)) and post-treated at 200 °C in N_2 atmosphere (Figure 4(b)) or at 500 °C in H_2S/Ar atmosphere (Figure 4(c)). Additionally, the relevant simulations were plotted with the measured XANES spectra. The Cu_2ZnSnS_4 nanoparticles used for these experiments were prepared by a one pot technique. The XANES spectra of the Cu_2ZnSnS_4 nanoparticle thin films were measured in the fluorescence mode as measurement in the transmission mode was not possible due to absorption by the substrate.

The spectrum of the as deposited Cu_2ZnSnS_4 nanoparticles showed some differences to the Cu_2ZnSnS_4 nanoparticle spectrum in Figure 2. For the nanoparticles from the one pot synthesis (Figure 4), the peak at 2470 eV (E_I) was less pronounced and a peak at 2481 eV (E_V) was found in contrast to the nanoparticles from colloidal synthesis (Figure 2). The reduced intensity of the peak at 2470 eV indicate less Cu/Zn in the native Sn site (2b), or vacancies and the peak at

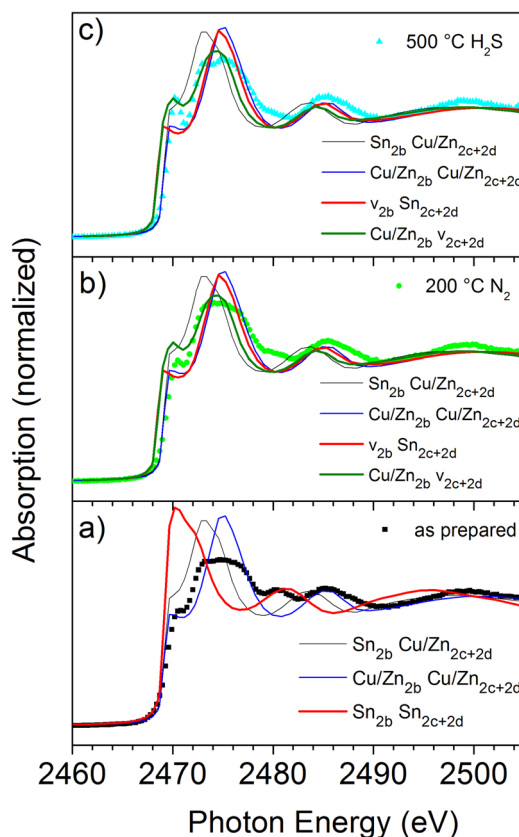


FIG. 4. Measured and simulated normalized XANES spectra at the S K-edge of (a) as prepared (black squares) and (b) annealed in N_2 atmosphere at 200 °C (green circles) and (c) in H_2S/Ar atmosphere (blue triangles) Cu_2ZnSnS_4 nanoparticle thin films. The measured XANES spectra are compared with different simulations.

2481 eV points towards some Sn in the 2c + 2d site, which is the native Cu and Zn site.

Heating at 200 °C under nitrogen atmosphere reduced the intensity of the peak at 2481 eV and slightly increased the intensity of the peak at 2470 eV. Therefore, heating at 200 °C mainly reduced the occupation of the 2c + 2d site with Sn atoms. The slight increase of the peak at 2470 eV can be either explained by an increase of Cu/Zn in the 2b site or a development of vacancies.

Upon heating at 500 °C in H₂S atmosphere, the intensity of the peak at 2481 eV decreased further while the intensity of the peak at 2470 eV increased strongly. Therefore, the occupation of the 2c + 2d site with Sn atoms was further decreased, but the major change was an increase of Cu/Zn in the 2b site or a development of vacancies.

Generally, a loss of Sn in Cu₂ZnSnS₄ nanoparticle films, in both the 2b and the 2c + 2d sites, took place upon heating. As the amount of Cu and Zn in the sample is not increased, the loss of Sn leaves vacancies. Whether the vacancies are only present in one of the lattice sites or in both the 2b and the 2c + 2d site, cannot be verified by XANES simulation.

By comparison of XANES measurements and simulations at the S K-edge, it has been shown that XANES is sensitive to Sn_{Cu/Zn} and Cu/Zn_{Sn} anti-site defects and vacancies. The occupation of lattice sites is dependent on both the synthesis method used and the treatment of nanoparticles.

XANES measurements and simulations point towards Cu/Zn anti-site defects on the intrinsic Sn (2b) position, or vacancies in colloidal synthesized Cu₂ZnSnS₄ nanoparticles. According to Walsh *et al.*,¹¹ the formation energies of most acceptor states are lower than the formation energies of donor states, resulting in a p-type material. This is also in accordance with surface photovoltage measurements of Cu₂ZnSn(S_xSe_{1-x})₄ layers.²³ In p-type Cu₂ZnSnS₄, the Sn vacancy has a much higher formation energy (~3 eV) than the Cu/Zn anti-site defect and the Cu/Zn vacancy, which have very similar formation energies (~1 eV). Therefore, the formation of Sn vacancies creating deep defects is quite unlikely. The Cu/Zn vacancy and the Zn anti-site defect create only shallow acceptor states. However, the Cu anti-site defect also creates a deep defect, which would limit the performance of solar cells.¹¹

The Sn_{Cu/Zn} anti-site defects observed for Cu₂ZnSnS₄ nanoparticles from the one-pot synthesis create deep defects (Sn_{Cu}) or donor states (Sn_{Zn}), which would be both unfavorable for p-type Cu₂ZnSnS₄ solar cells. However, these defects are easily reduced by annealing with 200 °C under nitrogen atmosphere. The strong increase of the peak at 2470 eV during heating at 500 °C under H₂S points towards a further loss of Sn at its native site. As the formation of an Sn vacancy is energetically unfavorable,¹¹ the loss of Sn is in all likelihood compensated by Zn and Cu on the native Sn site, resulting in Cu and Zn vacancies.

The measurements show that composition of the Cu₂ZnSnS₄ layer and the defect positions strongly depend on the treatments of the Cu₂ZnSnS₄ nanoparticle thin films. The monitoring of changes of the occupation of lattice sites due to annealing during the preparation of solar cells is an important issue. XANES can be used as a method for technology development by monitoring changes in the defect positions and correlating them to solar cell performances. Further experiments to correlate defects with solar cell performances are required.

The work was supported by the BMBF (Grant No. 03SF0363B). Muangjai Unruan, Atipong Bootchanont, Sukit Limpijumnong, and Wantana Klysuban are acknowledged for support with the XAS measurements and discussions. We are also grateful to the reviewer for suggesting a consideration of vacancies.

- ¹K. Ito and T. Nakazawa, *Jpn. J. Appl. Phys., Part 1* **27**, 2094 (1988).
- ²H. Katagiri, K. Jimbo, S. Yamada, T. Kamimura, W. Shwe Maw, T. Fukano, T. Ito, and T. Motohiro, *Appl. Phys. Express* **1**, 041201 (2008).
- ³D. Aaron, R. Barkhouse, O. Gunawan, T. Gokmen, T. K. Todorov, and D. B. Mitzi, *Prog. Photovoltaics* **20**, 6 (2012).
- ⁴S. Bag, O. Gunawan, T. Gokmen, Y. Zhu, T. K. Todorov, and D. B. Mitzi, *Energy Environ. Sci.* **5**, 7060 (2012).
- ⁵T. K. Todorov, J. Tang, S. Bag, O. Gunawan, T. Gokmen, Y. Zhu, and D. B. Mitzi, *Adv. Energy Mater.* **3**, 34 (2013).
- ⁶Q. Guo, G. M. Ford, W. C. Yang, B. C. Walker, E. A. Stach, H. W. Hillhouse, and R. Agrawal, *J. Am. Chem. Soc.* **132**, 17384 (2010).
- ⁷H. Katagiri, *Thin Solid Film* **480**, 426 (2005).
- ⁸H. Katagiri, K. Jimbo, W. S. Maw, K. Oishi, M. Yamazaki, H. Arikawa, and A. Takeuchi, *Thin Solid Film* **517**, 2455 (2009).
- ⁹K. Jimbo, R. Kimura, T. Kamimura, S. Yamada, W. S. Maw, H. Arikawa, K. Oishi, and H. Katagiri, *Thin Solid Films* **515**, 5997 (2007).
- ¹⁰K. Biswas, S. Lany, and A. Zunger, *Appl. Phys. Lett.* **96**, 201902 (2010).
- ¹¹A. Walsh, S. Chen, S.-H. Wei, and X.-G. Gong, *Adv. Energy Mater.* **2**, 400 (2012).
- ¹²G. P. Bernardini, D. Borroni, A. Caneschi, F. Di Benedetto, D. Gatteschi, S. Ristori, and M. Romanelli, *Phys. Chem. Miner.* **27**, 453 (2000).
- ¹³S. Schorr, H.-J. Hoebler, and M. Tovar, *Eur. J. Miner.* **19**, 65 (2007).
- ¹⁴T. Washio, H. Nozaki, T. Fukano, T. Motohiro, K. Jimbo, and H. Katagiri, *J. Appl. Phys.* **110**, 074511 (2011).
- ¹⁵S. R. Hall, J. T. Szymanski, and J. M. Stewart, *Can. Miner.* **16**, 131 (1978).
- ¹⁶J. Just, D. Lützenkirchen-Hecht, R. Frahm, S. Schorr, and T. Unold, *Appl. Phys. Lett.* **99**, 262105 (2011).
- ¹⁷C. Steinhagen, M. G. Pathani, V. Akhavan, B. Goodfellow, B. Koo, and B. A. Korgel, *J. Am. Chem. Soc.* **131**, 12554 (2009).
- ¹⁸X. Z. Lin, J. Kavalakatt, M. Lux-Steiner, and A. Ennaoui, in *Proceedings of 26th European Photovoltaics Solar Energy Conference, Hamburg, Germany, 5-8 September* (2011), pp. 2896–2899.
- ¹⁹J. J. Rehr, J. Mustre de Leon, S. I. Zabinsky, and R. C. Albers, *J. Am. Chem. Soc.* **113**, 5135 (1991).
- ²⁰A. L. Ankudinov, B. Ravel, J. J. Rehr, and S. D. Conradson, *Phys. Rev. B* **58**, 7565 (1998).
- ²¹X. Chen, H. Wada, A. Sato, and M. Mieno, *J. Solid State Chem.* **139**, 144 (1998).
- ²²J. T-Thienprasert, J. Nukeaw, A. Sungthong, S. Porntheeraphat, S. Singkarat, D. Onkaw, S. Rujirawat, and S. Limpijumnong, *Appl. Phys. Lett.* **93**, 051903 (2008).
- ²³X. Z. Lin, Th. Dittrich, S. Fengler, M. Ch. Lux-Steiner, and A. Ennaoui, *Appl. Phys. Lett.* **102**, 143903 (2013).